Cenozoic Deep-Sea Temperatures and Global Ice Volumes from Mg/Ca in Benthic Foraminiferal Calcite

C. H. Lear,* H. Elderfield, P. A. Wilson†

A deep-sea temperature record for the past 50 million years has been produced from the magnesium/calcium ratio (Mg/Ca) in benthic foraminiferal calcite. The record is strikingly similar in form to the corresponding benthic oxygen isotope ($\delta^{18}O$) record and defines an overall cooling of about 12°C in the deep oceans with four main cooling periods. Used in conjunction with the benthic $\delta^{18}O$ record, the magnesium temperature record indicates that the first major accumulation of Antarctic ice occurred rapidly in the earliest Oligocene (34 million years ago) and was not accompanied by a decrease in deep-sea temperatures.

Earth's climate is widely understood to have undergone dramatic changes over the past 100 million years (My) from the so-called mid-Cretaceous "greenhouse" to the late Cenozoic "icehouse" (*1, 2*). The long-term cooling over this period is thought to have resulted from a combination of factors that altered the amount and distribution of heat over Earth's surface. Variations in atmospheric greenhouse gases (principally CO_2), Earth's albedo, and linked changes in ocean-atmosphere circulation patterns, which are also influenced by the opening and closing of ocean gateways, could contribute to this long-term cooling. Yet, the relative importance of these different processes is uncertain and perhaps will remain so until detailed and unambiguous records of global temperature are available.

Many proxy records have been developed to define the timing and magnitude of global climate change during the Cenozoic. Arguably, the most established and reliable of these records is that derived from the oxygen isotopic composition ($\delta^{18}O$) of benthic foraminiferal calcite obtained from deep-sea cores (*1, 2*). The power of this particular record lies in the fact that the deep ocean is insulated from large seasonal, latitudinal, and geographical variations in temperature and salinity and therefore is more representative of global change than surface ocean or continental records are. The form of this deep-sea benthic $\delta^{18}O$ record is particularly well constrained for the past 50 My and is composed of a series of abrupt short-term (~1 My) "steplike" increases superimposed on a long-

er term increase. However, $\delta^{18}O$ values of marine carbonates are controlled by the temperatures and isotopic compositions of the seawater ($\delta^{18}O_{sw}$) from which they formed. If an independent record of deep-sea temperature was available, this complexity in the benthic foraminiferal calcite $\delta^{18}O$ record could be an important advantage because $\delta^{18}O_{sw}$ in the deep oceans primarily records global continental ice volume.

Attempts to extract global ice budgets from deep-sea $\delta^{18}O$ records by indirect methods have yielded very different estimates of the timing of the onset of the accumulation of continental-scale ice sheets. These range from the Early Cretaceous [~150 million years ago (Ma)] (*3*) to the Middle Miocene (~15 Ma) (*1*), but recent improvements in the stratigraphic resolution of the $\delta^{18}O$ record have led to suggestions that either the late Middle Eocene (~43 Ma) or the earliest Oligocene (34 Ma) is a better estimate of the initiation of major ice sheets within the Cenozoic (*4*). Supporting evidence for this interpretation comes from oceanic records of ice-rafted debris, weathered clay mineral compositions, microfossil assemblages, sea level changes, and hiatuses (*5*), but such records are often incomplete and ambiguous and do not allow ice volumes to be estimated or the causes of their expansion and contraction to be evaluated. Here, we present a low-resolution deep-sea temperature record for the past 50 My, using Mg/Ca in benthic

foraminiferal calcite. We use this record to extract the $\delta^{18}O_{sw}$ component from the benthic foraminiferal $\delta^{18}O$ record and thus define global continental ice volume.

Mg/Ca Paleothermometry

The basis for the Mg/Ca paleothermometry method lies in laboratory experiments that show that the partition coefficient of Mg^{2+} into inorganic calcite correlates strongly with temperature (*6*) and in empirical and culture studies of temperature-dependent uptake of Mg in marine biogenic calcites (*7, 8*). Mg/Ca of planktonic foraminiferal calcite has been used to estimate Quaternary sea surface temperatures (*9*). An empirical Mg/Ca–temperature calibration for a modern species of benthic foraminifera, *Cibicidoides floridanus*, also exists (*10*) and has been used to determine Quaternary deep-sea temperatures (*11*).

We measured Mg/Ca in six species of benthic foraminifera of late Cenozoic age (~50 to 0.5 Ma) from three deep-sea drilling sites in the Pacific, Atlantic, and Southern oceans in order to generate a low-resolution record (about two samples per 1 My). We also generated a high-resolution record (~25 samples per 1 My) across the Eocene-Oligocene boundary (Table 1) (*12*).

In order to generate a temperature record from the Mg/Ca data, four issues must be addressed. The first is that of interspecific differences in Mg/Ca (Fig. 1A). Such differences are common in $\delta^{18}O$ records (*1*), and our data show that the same is true for Mg/Ca (Fig. 1A). The reasons for these offsets in Mg/Ca are unclear. Therefore, we followed the procedure by which $\delta^{18}O$ records are generated and applied a simple species adjustment to our Mg/Ca data by normalizing all species to *Oridorsalis umbonatus* (*13*). A smoothed form of this species-adjusted record is presented in Fig. 1B.

The second issue is to assess the preservation of primary Mg/Ca values. Benthic foraminifera are generally thought to have higher preservation potential than planktonic foraminifera, and three lines of evidence indicate that the trend shown by the Mg/Ca data represents a primary signal. (i) Depth profiles of interstitial waters of deep-sea sediments show trends of increasing Ca and decreasing Mg with depth, caused by chemical transport between the ocean and the basalts underlying the sediment column. Postdepositional re-

Department of Earth Sciences, University of Cambridge, Downing Street, Cambridge CB2 3EQ, UK.

*To whom correspondence should be addressed. E-mail: chl26@esc.cam.ac.uk
†Present address: School of Ocean and Earth Sciences, Southampton Oceanography Centre, European Way, Southampton, SO14 3ZH, UK.

Table 1. Locations of deep-sea sites and age ranges of analyzed samples.

Site	Location	Water depth (m)	Age of samples (Ma)	Paleowater depth (m)
DSDP 522	26.11°S, 05.13°W	4400	32 to 35	3000
DSDP 573	0.50°N, 133.31°W	4300	0 to 35	4300 to 3000
ODP 689	64.52°S, 03.10°E	2080	37 to 48	1500
ODP 926	03.72°N, 42.91°W	3600	6 to 12	3500

crystallization of calcite as it reequilibrates with surrounding pore waters should therefore tend to lower the calcite Mg/Ca (*14*). This diagenetic process should be more enhanced in older samples, yet data show a trend of increasing Mg/Ca with age (the effect of burial temperature on Mg of any recrystallized calcite will be trivial). (ii) Diagenesis should cause chemical homogenization of all coexisting biogenic calcite, yet consistent interspecific differences persist over the whole record (Fig. 1A). (iii) Diagenesis should cause homogenization of the chemical composition of individual foraminiferal shells. However, electron microprobe analyses of individual benthic foraminifera (*Nuttallides truempyi*) show that concentrations of trace elements vary substantially within an individual test. This heterogeneity

is unrelated to test structures and porosity, and the range in concentration within an individual test is unrelated to the mean concentration of the test, suggesting that lower concentrations are not the result of recrystallization. Examination of cleaned shells under a scanning electron microscope revealed no secondary calcite, such as coccoliths or calcite rhombs.

The third requirement to determine temperatures from Mg/Ca data is to know past seawater Mg/Ca. No independent proxy record exists for secular variation in seawater Mg/Ca. However, the fluxes of Mg^{2+} and Ca^{2+} into and out of the modern oceans are reasonably well constrained (*15*) and have been used, together with certain key geological parameters (for example, records of oceanic crustal cycling and dolomite abundance), to develop simple geochemical

models that estimate past seawater Mg/Ca (*16, 17*). The resultant temperature record is not very sensitive to the choice of model, and we used that of (*16*), which includes a comprehensive treatment of dolomite cycling and has the advantage of predicting realistic deep-sea Pleistocene temperatures from our Mg/Ca data.

Finally, in order to translate Mg/Ca records into temperatures, a calibration is required. We used the published (*10*) modern Mg/Ca temperature calibration from *C. floridanus* and applied a species adjustment to our reference species, *O. umbonatus*, by changing the preexponential constant of the Mg temperature calibration so as to match Mg/Ca and $\delta^{18}O$ temperatures in an ice-free world [$\delta^{18}O_{sw} = -1.2$ per mil, which we assumed to be the case between 48 and 49 Ma (*18*)]. The Mg temperature record constructed on
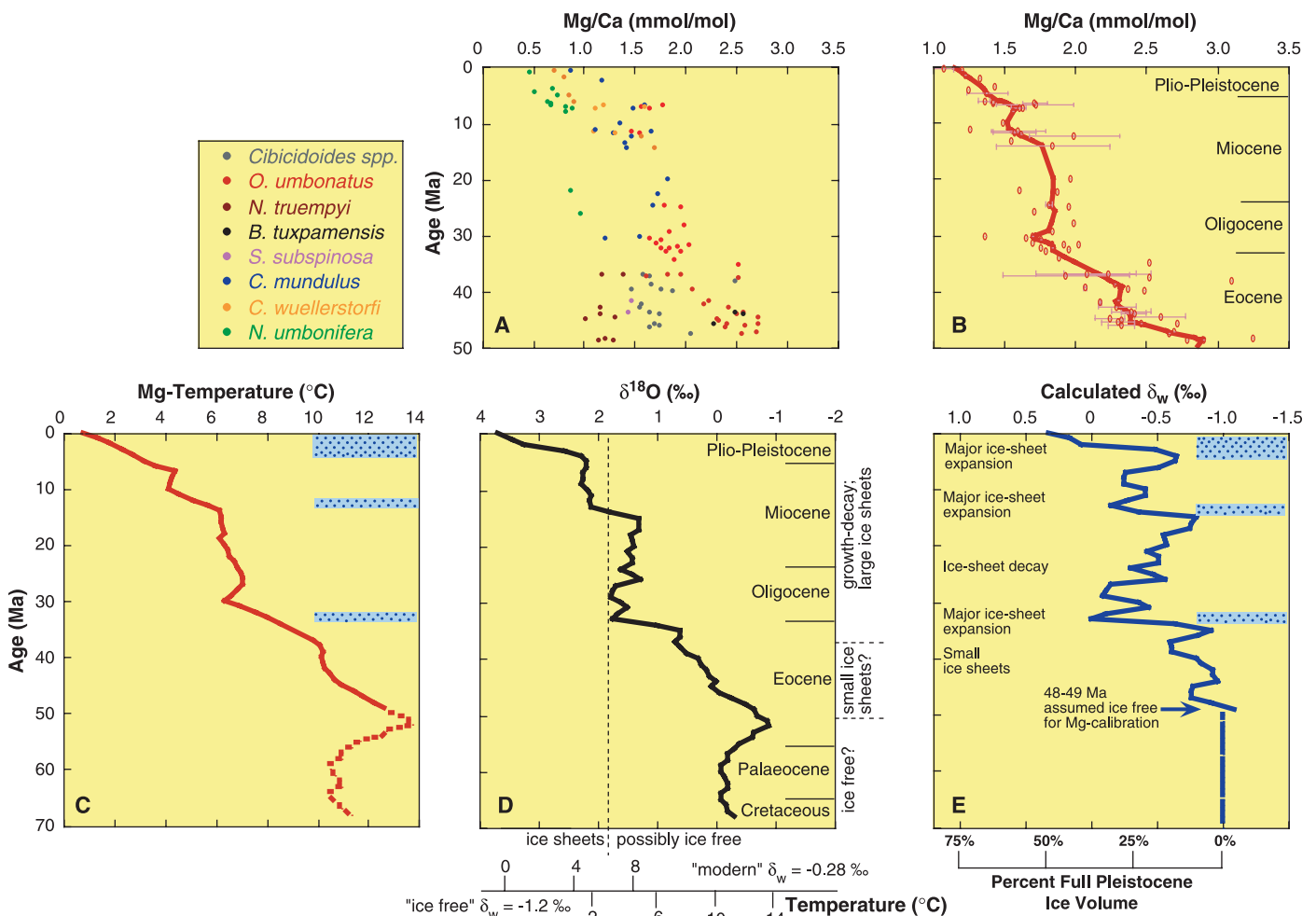

Fig. 1. (**A**) Composite multispecies benthic foraminiferal Mg/Ca records from three deep-sea sites: DSDP Site 573, ODP Site 926, and ODP Site 689. (**B**) Species-adjusted Mg/Ca data. Error bars represent standard deviations of the means where more than one species was present in a sample. The smoothed curve through the data represents a 15% weighted average. (**C**) Mg temperature record obtained by applying a Mg calibration to the record in (B). Broken line indicates temperatures calculated from the $\delta^{18}O$ record assuming an ice-free world. Blue areas indicate periods of substantial ice-sheet growth determined from the $\delta^{18}O$ record in conjunction with the Mg temperature. (**D**) Cenozoic composite benthic foraminiferal $\delta^{18}O$ record based on Atlantic cores and normalized to *Cibicidoides spp.* from Miller *et al.* (*2*). Vertical dashed line indicates probable existence of ice sheets as estimated by (*2*). ‰, per mil; δ_w, seawater $\delta^{18}O$. (**E**) Estimated variation in $\delta^{18}O$ composition of seawater, a measure of global ice volume, calculated by substituting Mg temperatures and benthic $\delta^{18}O$ data into the $\delta^{18}O$ paleotemperature equation (Eq. 2). The volume of "full Pleistocene glacial ice volume" is from Dwyer *et al.* (*7*). All records are plotted to the time scale of Berggren *et al.* (*34*).

this basis (Fig. 1C) shows a consistent long-term decrease in deep-ocean temperature of ~12°C over the past 50 My. Moreover, the overall form of this curve is remarkably similar to the corresponding composite benthic $\delta^{18}O$ record (Fig. 1D).

Figure 1A shows scatter that interspecific normalization cannot fully eliminate and that must be addressed in order to refine the Mg-based paleotemperature record. One difficulty is that of natural heterogeneity in shell chemistry, which is exacerbated by the analysis of small numbers of individuals in a small size fraction (19). The application of Mg/Ca paleothermometry to longer time scales introduces new problems (for example, diagenesis and changes in seawater Mg/Ca), which we have addressed, and uncertainties that remain in applications within Quaternary paleoceanography. New Mg/Ca temperature calibrations for benthic foraminifera are urgently required.

Cenozoic Cooling

The temperature record shows a general cooling trend for the past 50 My, but its resolution is too low to define abrupt temperature extremes. Assuming that the process of deep water formation at high latitudes prevailed throughout the past 50 My, these deep-ocean temperatures can be inferred to represent polar surface temperatures (1). The temperature trend (Fig. 1C) appears to comprise four main cooling phases separated by periods of more stable temperatures. These cooling phases occur during the early Middle Eocene, the Late Eocene through Early Oligocene, the late Middle Miocene, and the Plio-Pleistocene.

Alternative evidence supports the existence of these principal cooling phases. A sharp cooling in the early Middle Eocene has been invoked to explain the abundance of siliceous sediments of this age (20). The Early Eocene warm climate is thought to have promoted intense chemical weathering of siliceous rocks at high latitudes, which resulted in high concentrations of dissolved silica in the oceans. The subsequent cooling stimulated upwelling of nutrient-rich water and intense biosilicification. The cooling over the Late Eocene through Early Oligocene is coincident with the transition from "Paleogene" to "transitional" benthic foraminiferal faunas and high extinction rates in planktonic and terrestrial faunas. The initiation of this deep water cooling also coincides with a reduction in the extent of tropical rainforests on land (21, 22). The cooling in the late Middle Miocene is marked by a narrowing of tropical and warm subtropical biotic provinces in terrestrial and marine environments (23). Warmwater diatom assemblages were replaced by cold-water species at this time (24). The Plio-Pleistocene cooling is not represented by an extinction phase in benthic foraminiferal faunas; instead, faunal groups adapted to the changing bottom water conditions by migration (21).

Global Ice Volumes

Our deep-sea temperature record enables the $\delta^{18}O_{sw}$ component of the benthic $\delta^{18}O$ record to be calculated (Fig. 1E). This approach has been successfully applied to ostracode Mg/Ca records of Late Pliocene and Quaternary age (7). In principle, therefore, both the timing of initiation of continental ice accumulation and its record through the Cenozoic can be determined. However, extreme values of $\delta^{18}O_{sw}$ will not be represented because this record was compiled with smoothed $\delta^{18}O$ and Mg temperature records. Nevertheless, three main rapid ice-accumulation events are depicted: (i) the earliest Oligocene (Oi-1) (25), (ii) the late Early Miocene, and (iii) the Pliocene through Pleistocene. Each $\delta^{18}O_{sw}$ event corresponds to a rapid excursion (~1 per mil) in the global benthic $\delta^{18}O$ records, and all are generally thought to be associated with a rapid accumulation of continental ice that, in turn, has been attributed to threshold levels in the climate system attained by the application of gradual forcing mechanisms (26, 27).

Perhaps the best known example of such an event is the positive $\delta^{18}O$ excursion in earliest Oligocene time (Oi-1) (25, 28). This excursion was first ascribed to a 5°C temperature drop associated with the onset of thermohaline circulation (26). More recently, Oi-1 has been associated with the onset of continental ice accumulation on Antarctica (27, 28).

Therefore, we generated a high-resolution Mg/Ca paleotemperature record for this event to use in conjunction with a benthic $\delta^{18}O$ record (28) to calculate $\delta^{18}O_{sw}$ over this period (Fig. 2). Our data confirm that most of the benthic $\delta^{18}O$ signal results from a buildup of continental ice with little temperature response. This conclusion is in accord with faunal studies of benthic foraminifera, which document gradual, stepped ex-
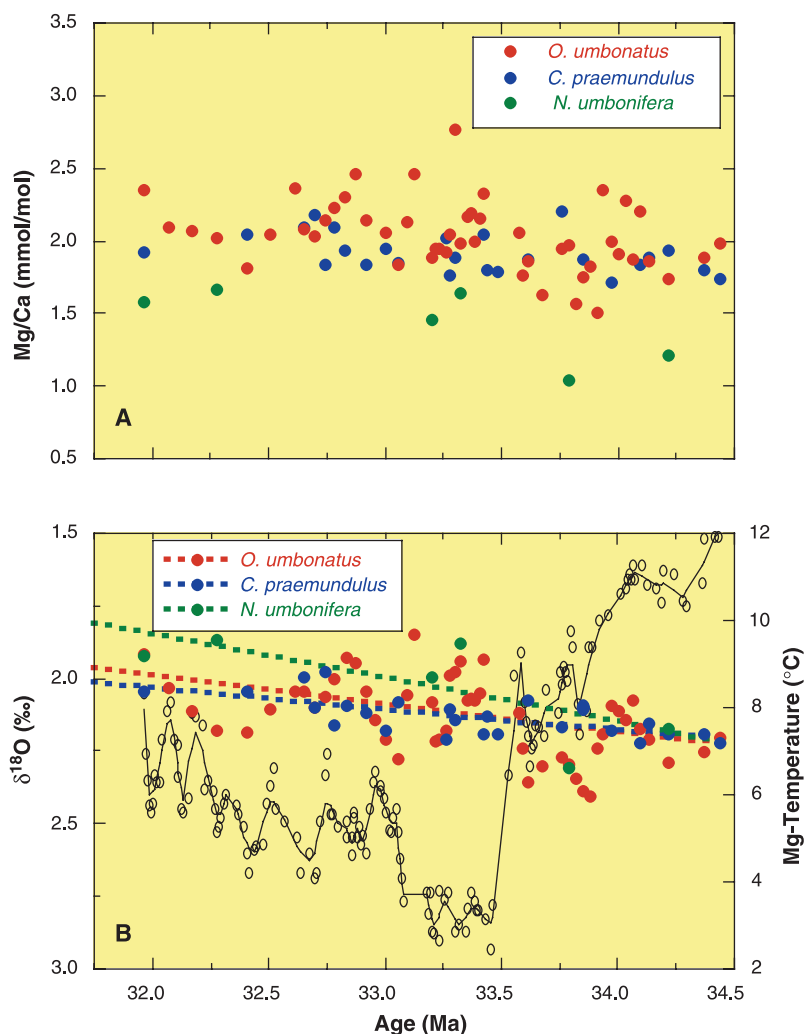

Fig. 2. (**A**) Mg/Ca of three species of benthic foraminifera (not normalized) across the Eocene-Oligocene boundary (DSDP Site 522). (**B**) Mg temperatures calculated from Mg/Ca normalized to *O. umbonatus* (solid symbols) and $\delta^{18}O$ of *Gyroidinoides spp.* (open symbols) from Zachos *et al.* (27) through the first major $\delta^{18}O$ excursion of the Cenozoic (Oi-1). Mg temperatures of *O. umbonatus* and the $\delta^{18}O$ record represent a three-point moving average of the data.

tinctions from the Middle Eocene to Late Oligocene, with no clear extinction event corresponding to Oi-1 (*29*). Further refinement of the Mg temperature calibration may change the predicted temperatures somewhat (and hence absolute ice volume) across this event. But, the lack of a deep-sea temperature decline implies rapid ice accumulation during Oi-1 without a concomitant decrease in polar surface temperatures. Perhaps, rather than excess warmth, a lack of moisture available for snow precipitation on Antarctica prevented ice accumulation immediately before this time. Elsewhere, it has been suggested that the new moisture source could have been provided by the opening of a seaway between Antarctica and Australia, thereby reducing the aridity of the polar region (*30*). The lithostratigraphic results of recent drilling [Ocean Drilling Program (ODP) Site 1182] in the Australian-Antarctic seaway has confirmed a switch from early-rift clastic deposition to carbonate deposition in the Late Eocene and the deposition of a 20-m-thick nanofossil chalk bed in the earliest Oligocene (*31*). The age of this marine deposit lends support to the hypothesis that opening of the seaway played an integral part in the initiation of continental-scale ice sheets, perhaps by making Antarctica a continent with a less arid maritime climate.

The large accumulation of ice in the late Middle Miocene (~14 Ma) has been associated with East Antarctic Ice Sheet growth (*32*). Our Mg/Ca data do not cover this event in any detail but indicate that most (~85%) of the benthic $\delta^{18}O$ increase at this time can be attributed to an increase in continental ice volume; the rest of the increase reflects a cooling of bottom waters. The last of the rapid shifts in the Cenozoic benthic $\delta^{18}O$ record reflects the Pleistocene glaciation of the Northern Hemisphere (*1, 33*). The Mg temperature record suggests that about two-thirds of the increase in benthic foraminiferal $\delta^{18}O$ over the past 4 My can be attributed to the accumulation of continental ice.

The deep-sea temperature record from Mg/Ca in benthic foraminiferal calcite suggests a cooling of ~12°C over the past 50 My. Four phases of cooling support the hypothesis that many benthic faunal turnovers coincide with times of temperature decline. Used in conjunction with a benthic $\delta^{18}O$ record, the Mg temperature record provides estimates of global ice volume. The findings suggest that the first major continental-scale ice accumulation occurred in the earliest Oligocene. A high-resolution study shows that this event was not marked by a decrease in deep-sea temperature. This suggests that a mechanism other than temperature decline must have promoted the initiation of Antarctic ice.

References and Notes

1. N. J. Shackleton and J. P. Kennett, *Initial Rep. Deep Sea Drill. Proj.* **29**, 743 (1975).
2. K. G. Miller, R. G. Fairbanks, G. S. Mountain, *Paleoceanography* **2**, 1 (1987).
3. R. K. Matthews and R. Z. Poore, *Geology* **8**, 501 (1980).
4. N. J. Shackleton, *Palaeogeogr. Palaeoclimatol. Palaeoecol.* **57**, 91 (1986); J. C. Zachos, L. D. Stott, K. C. Lohmann, *Paleoceanography* **9**, 353 (1994).
5. J. P. Kennett and P. F. Barker, *Proc. Ocean Drill. Program Sci. Results* **113**, 937 (1990); W. U. Ehrmann and A. Mackensen, *Palaeogeogr. Palaeoclimatol. Palaeoecol.* **93**, 85 (1992); J. V. Browning, K. G. Miller, D. K. Pak, *Geology* **24**, 639 (1996).
6. A. Katz, *Geochim. Cosmochim. Acta* **37**, 1563 (1973); E. A. Burton and L. M. Walter, *Geochim. Cosmochim. Acta* **55**, 777 (1991); G. Hartley and A. Mucci, *Geochim. Cosmochim. Acta* **60**, 315 (1996).
7. G. S. Dwyer *et al.*, *Science* **270**, 1347 (1995).
8. T. Mitsuguchi, E. Matsumoto, O. Abe, T. Uchida, P. J. Isdale, *Science* **274**, 961 (1996); D. Nürnberg, J. Bijma, C. Hemleben, *Geochim. Cosmochim. Acta* **60**, 803 (1996).
9. D. W. Hastings, A. D. Russell, S. R. Emerson, *Paleoceanography* **13**, 161 (1998); T. Mashiotta, D. W. Lea, H. J. Spero, *Earth Planet. Sci. Lett.* **170**, 417 (1999).
10. Y. Rosenthal, E. A. Boyle, N. Slowey, *Geochim. Cosmochim. Acta* **61**, 3633 (1997).
11. P. A. Martin, D. W. Lea, Y. Rosenthal, T. P. Papenfuss, M. Sarnthein, paper presented at the 6th International Conference on Paleoceanography, Lisbon, 23 to 28 August 1998.
12. K. J. Hsü *et al.*, *Init. Rep. Deep Sea Drill. Proj.* **73**, 187 (1984); L. Mayer *et al.*, *Init. Rep. Deep Sea Drill. Proj.* **85**, 137 (1985); P. F. Barker *et al.*, *Proc. Ocean Drill. Program Initial Rep.* **113**, 89 (1988); N. J. Shackleton *et al.*, *Proc. Ocean Drill. Program Initial Rep.* **154**, 153 (1995). Table 1 shows locations of the deep-sea sites, with an age range of the analyzed samples. An average of six benthic foraminifera (>125-μm size fraction) was crushed between glass plates before ultrasonication in water and methanol, oxidation (boiled for 10 min in 30% H_2O_2 + 0.1 M NaOH), and leaching in weak acid (0.001 M HNO_3) for 30 s. The samples were then dissolved in quartz-distilled 0.075 M HNO_3 before analysis for Mg/Ca by inductively coupled plasma–atomic emission spectrometry. This method gives precisions of 0.3 to 0.5% relative standard deviation. Mg/Ca data are available at www.sciencemag.org/feature/data/1045633.shl.
13. All species were normalized to *O. umbonatus* because this species is present in all four sites studied. Mg/Ca offsets for species coexisting with *O. umbonatus* in samples from ODP Sites 689 and 926 were calculated from the differences between whole-core means of the species. However, *O. umbonatus* from the Deep Sea Drilling Project (DSDP) Site 573 was not generally present with other species. Offsets were therefore calculated by extrapolating the DSDP Site 573 data to zero age, using lines of best fit. These values were averaged with those from ODP Site 926. The offsets obtained for *C. wuellerstorfi* from different ages varied, and an average was used. The following adjustments (in millimoles per mole) were made to the raw data: *C. praemundulus*, +0.10; *N. umbonifera*, +0.75; *C. wuellerstorfi*, +0.43; *C. mundulus*, +0.15; *N. truempyi*, +1.16; *Cibicidoides spp.*, +0.61; *Stilostomella subspinosa*, +0.90; and *Bulimina tuxpamensis*, −0.09.
14. J. M. Gieskes, in *Chemical Oceanography*, J. P. Riley and R. Chester, Eds. (Academic Press, London, 1983), vol. 8, pp. 221–269.
15. Mg and Ca resulting from weathering processes are transferred from the continent to the ocean by rivers. Submarine hydrothermal processes remove some of this Mg by exchange for Ca from the oceanic crust. Therefore, Ca from rivers and hydrothermal sources is removed only during carbonate deposition, whereas Mg, derived only from rivers, is removed during dolomite production and hydrothermal activity [(*21*); J. I. Drever *et al.*, in *Chemical Cycles in the Evolution of the Earth*, C. B. Gregor *et al.*, Eds. (Wiley, New York, 1988), pp. 17–53].
16. B. H. Wilkinson and T. J. Algeo, *Am. J. Sci.* **289**, 1158 (1989).
17. L. A. Hardie, *Geology* **24**, 279 (1996).
18. The calibration equation for *C. floridanus* (*9*) was modified to take account of species differences (factor *f*) and temporal variations in seawater Mg/Ca as

$$Mg/Ca = 1.36f \left[\frac{(Mg/Ca)_{sw-t}}{(Mg/Ca)_{sw-0}} \right] \times 10^{0.044T} \quad (1)$$

Where the subscripts refer to seawater today (sw-0) and at time *t* (sw-*t*). $(Mg/Ca)_{sw-t}$ was derived from (*16*). The factor *f* was determined by solving Eq. 1 at 48 to 49 Ma with average benthic Mg/Ca and temperatures derived from the $\delta^{18}O$ paleotemperature equation [N. J. Shackleton, *Cent. Natl. Rech. Sci. Colloq. Int.* **219**, 203 (1974)].

$$T = 16.9 - 4.0(\delta^{18}O_c - \delta^{18}O_{sw}) \quad (2)$$

assuming an ice-free world where $\delta^{18}O_{sw} = -1.2$ per mil (*1*). A species offset of +0.5 per mil is applied to the $\delta^{18}O_c$ data of (*2*), which has been normalized to *Cibicidoides* [N. J. Shackleton *et al.*, *Initial Rep. Deep Sea Drill. Proj.* **74**, 599 (1984)].
19. Interspecific differences occur for Mg/Ca and Sr/Ca in benthic foraminifera [H. Elderfield, C. J. Bertram, J. Erez, *Earth Planet. Sci. Lett.* **142**, 409 (1996)], and the work on Sr/Ca shows that the relative standard deviation on analysis of individuals increases dramatically with decreasing size (for example, 2.8% for 500 μm to 7.3% for 250 μm). With standard deviations in Fig. 1A of ~0.2 for some species, the 1σ SE on an analysis of *n* individuals (0.2/*n*) is such that ~25 individuals, or a 50% increase in the size of individuals analyzed, would be needed to halve the 1σ SE of the analysis.
20. B. McGowran, *Geology* **17**, 857 (1989).
21. E. Thomas, *The Antarctic Paleoenvironment: A Perspective on Global Change, Part One*, vol. 56 of *Antarctic Research Series*, J. P. Kennett and D. A. Warnke, Eds. (American Geophysical Union, Washington, DC, 1992), pp. 141–165.
22. D. R. Prothero, *The Eocene-Oligocene Transition: Paradise Lost* (Columbia Univ. Press, New York, 1994).
23. J. A. Wolfe, *The Carbon Cycle and Atmospheric CO₂: Natural Variations Archean to Present*, vol. 32 of *Geophysical Monograph Series*, E. T. Sundquist and W. S. Broecker, Eds. (American Geophysical Union, Washington, DC, 1985), pp. 357–375; B. P. Flower and J. P. Kennett, *Palaeogeogr. Palaeoclimatol. Palaeoecol.* **108**, 537 (1994).
24. I. Koizumi, *Palaeogeogr. Palaeoclimatol. Palaeoecol.* **77**, 181 (1990).
25. K. G. Miller, J. D. Wright, R. G. Fairbanks, *J. Geophys. Res.* **96**, 6829 (1991).
26. J. P. Kennett and N. J. Shackleton, *Nature* **260**, 513 (1976).
27. J. C. Zachos, K. C. Lohmann, J. C. G. Walker, S. W. Wise, *J. Geol.* **101**, 191 (1993).
28. J. C. Zachos, T. M. Quinn, K. A. Salamy, *Paleoceanography* **11**, 251 (1996).
29. E. Thomas, in *Eocene-Oligocene Climatic and Biotic Evolution*, D. R. Prothero and W. A. Berggren, Eds. (Princeton Univ. Press, Princeton, NJ, 1992), pp. 245–271.
30. L. R. Bartek, L. C. Sloan, J. B. Anderson, M. I. Ross, in *Eocene-Oligocene Climatic and Biotic Evolution*, D. R. Prothero and W. A. Berggren, Eds. (Princeton Univ. Press, Princeton, NJ, 1992), pp. 131–159.
31. A. Hine *et al.*, *Eos Trans. Am. Geophys. Union* **80**, 521 (1999).
32. B. P. Flower and J. P. Kennett, *Paleoceanography* **10**, 1095 (1995).
33. G. H. Haug and R. Tiedemann, *Nature* **393**, 673 (1998).
34. W. A. Berggren, D. V. Kent, C. C. Swisher, M.-P. Aubry, *Soc. Econ. Paleontol. Mineral. Spec. Publ.* **54**, 129 (1995).
35. We thank E. Thomas for her very generous help in taxonomy and provision of samples, J. Zachos for provision of $\delta^{18}O$ data from DSDP Site 522, K. Miller for provision of the composite benthic $\delta^{18}O$ curve with adjusted age model, and the ODP for samples. Financial support for this research was provided by National Environment Research Council grants GT04/97/ES/46 (C.H.L.) and GST/02/1823 (H.E.).